Electronic Supplementary Material (ESI) for Dalton Transactions.

Supporting Information

Ga^{III}triarylcorroles with Push-Pull Substitutions: Synthesis, Electronic Structure and Biomedical Applications

Yingjie Niu [a,#], Lin Wang[b,#], Yingxin Guo,[c] Weihua Zhu,[a] Rodah C. Soy,[d] Balaji Babu,[d] John Mack,*[,d] Tebello Nyokong,[d] Haijun Xu*[,c] and Xu Liang*[,a]

a. School of Chemistry and Chemical Engineering, Jiangsu University, Zhenjiang 212013, P. R. China.
b. Affiliated Hospital of Jiangsu University, Jiangsu University, Zhenjiang 212013, P. R. China
c. Jiangsu Co-Innovation Center of Efficient Processing and Utilization of Forest Resources, College of Chemical Engineering, Nanjing Forestry University, Nanjing 210037, P. R. China.
d. Institute for Nanotechnology Innovation, Department of Chemistry, Rhodes University, Makhanda 6140, South Africa.

E-mail: liangxu@ujs.edu.cn (to Prof. Dr Xu Liang); xuhaijun@njfu.edu.cn (to Prof. Dr Haijun Xu); j.mack@ru.ac.za (to Prof. Dr John Mack)

#: These two authors were contributed equally.

Contents

1. Experimental Details

1.1 General

All reagents and solvents were purchased from Sigma Aldrich or Aladdin Reagents and used as supplied unless otherwise described. All solvents used were of analytical grade and were purified and dried by routine procedures immediately before use. Neutral silica was prepared by adding a few drops of triethylamine to the slurry. Chemicals and reagents used for cellular uptake, *in vitro* dark cytotoxicity and PDT studies such as Triton-100 X, ethylenediaminetetraacetic acid (EDTA), Dulbecco's phosphate-buffered saline (DPBS), trypan blue, Dulbecco's modified Eagle's media (DMEM) and trypsin were obtained from Sigma-Aldrich. The MTT assay was purchased from Sigma-Aldrich. Cultures of the human breast adenocarcinoma Michigan cancer-7 (MCF-7) cell line were obtained from Cellonex®. 10% (v/v) heat-inactivated fetal calf serum (FCS), and 100 unit/mL penicillin-100 µg/mL streptomycin-amphotericin B were obtained from Lonza (Biowest®). Dulbecco's phosphate-buffered saline (DPBS) and Dulbecco's modified Eagle's medium (DMEM) were purchased from Lonza®. *Escherichia coli* (ATCC 25922) was obtained from Microbiologics, and *Staphyloccocus aureus* (ATCC 25923) was obtained from Davies Diagnostics, South Africa. Nutrient agar and bacteriological BBL® Mueller Hinton broth for the PACT studies on planktonic cells were purchased from Merck and prepared according to the manufacturer's specifications. The crystal violet assay and tryptic soy broth for the PACT studies on biofilm cells were purchased from Sigma-Aldrich. Phosphate buffer saline (PBS 10 mM, pH 7.4) was prepared by the standard procedure with 10 mM $NaHPO_4$, 137 mM NaCl, 1.8 mM KH_2PO_4 and 2.7 mM KCl in 1 L of type II Millipore water collected from an ELGA, Veolia water PURELAB, flex system (Marlow, UK).

High-resolution mass spectra (HRMS) data were obtained on an LTQ Orbitrap XL spectrometer in ESI mode. MALDI-TOF-mass spectra were recorded on a Bruker AutoFLEX III Smartbeam TOF/TOF mass spectrometer, while ^1H NMR spectra were obtained from Bruker 400 or 600 MHz spectrometers with $CDCl_3$ (δ = 7.26 ppm) or trimethylsilane used as an internal reference. Triplet state lifetimes were determined in nitrogen saturated DMSO solution at 500 nm by using an Edinburgh Instruments LP980 spectrometer and a pump beam of 425 nm provided by an Ekspla NT-342B laser (2.0 mJ/7

ns, 20 Hz). FTIR-spectra were recorded on a Nicolet Nexus 470 FT-IR spectrophotometer, and UV-Vis absorption spectra were measured with Shimadzu UV3600 and UV2550 spectrophotometers. The fluorescence spectra were obtained using a Cary Eclipse fluorescence spectrophotometer (Varian Australia). Fluorescence lifetimes were measured by time-correlated single-photon counting (TCSPC) (FluoTime 300, Picoquant GmbH) with a diode laser (LDH-P-420, Picoquant_GmbH, 20 MHz repetition rate, 44 ps pulse width).

1.2 Synthetic details

1.2.1 Synthesis of H_3triarylcorrole C-1. Pentafluorodipyrromethane **1** (6.0 mmol, 1.87 g) and9-(4-formylphenyl)-3,6-di-*t*-butyl-9H-carbazole **2** (2.0 mmol, 767.3 mg), were dissolved in 140 mL freshly distilled dry CH_2Cl_2, and the mixture was stirred at room temperature for 20 min in the absence of light under Ar. Then, a catalytic amount of trifluoroacetic acid was added (0.54 mmol, 40 μL) and the mixture was continually stirred for 4.5h. After the mixture was diluted to 600 mL (CH_2Cl_2), an excess amount of DDQ was added (7.7 mmol, 1.8 g) and further stirred for about 0.5 h. After removal of organic solvent, the residue was purified by silica gel column chromatography (200-300 mesh; eluent, 1:1 CH_2Cl_2:hexane (v:v)) to give the pure target compound in a 17.0% yield (303.2 mg). UV-vis (CH_2Cl_2), λ_{max} / nm (log ε): 417 (5.07). ^{1}H NMR ($CDCl_3$, 600 MHz) δ_H 9.13 (d, J = 6.0 Hz, 2H), 8.86 (d, J = 7.6 Hz, 2H), 8.79 (d, J = 6.6 Hz, 2H), 8.59 (s, 2H), 8.41−8.37 (m, 2H), 8.27 (d, J = 2.4 Hz, 2H), 7.98 (d, J = 7.8 Hz, 2H), 7.77−7.79 (m, 2H), 7.65−7.62 (m, 2H), 1.55 (s, 18H) ppm. High-Resolution ESI-MS (negative): m/z = 982.2920 (Calcd for $C_{57}H_{38}F_{10}N_5$ $[M-H]^-$ = 982.2962).

1.2.2 Synthesis of Ga^{III}triarylcorrole G-1. H_3triarylcorrole **C-1** (98.39 mg, 0.1 mmol) and $GaCl_3$ (0.176 g, 1 mmol) were dissolved in 20 mL dry pyridine, stirred and refluxed at 140°C in the absence of light under Ar. After removal of the organic solvent, the residue was purified by silica gel column chromatography (200−300 mesh; eluent, 1:1 CH_2Cl_2:hexane; v:v) to give the pure target compound in 58.0% yield (63.4 mg). UV-vis (CH_2Cl_2), λ_{max} / nm (log ε): 424 (5.01). ^{1}H NMR ($CDCl_3$, 600 MHz) δ_H 9.25 (d, J = 3.6 Hz, 2H), 8.96 (d, J = 4.2 Hz, 2H), 8.89 (d, J = 4.2 Hz, 2H), 8.81 (d, J = 4.2 Hz, 2H), 8.34 (d, J = 8.4 Hz, 2H), 8.25 (d, J = 1.8 Hz, 2H), 7.93 (d, J =8.4 Hz, 2H), 7.75 (d, J = 8.4 Hz, 2H), 7.62-7.61 (m, 2H), 6.67 (t,

J = 7.8 Hz, 1H), 5.87 (t, J = 7.2 Hz, 2H), 2.93 (d, J = 5.42 Hz, 2H),1.54 (s, 18H) ppm. High-Resolution ESI-MS (negative): m/z = 1128.2543 (Calcd for $C_{62}H_{41}F_{10}GaN_6$ $[M]^-$ = 1128.2483). Elemental analysis: Calcd. for $C_{62}H_{41}F_{10}GaN_6$, C, 65.92; H, 3.66; F, 16.82; N, 7.44; Found, C, 66.12; H, 3.81; N, 7.28.

1.2.3 Synthesis of H_3triarylcorrole C-2. The general synthetic procedure is similar with that of **C-1** except *N*-butyl-4-carbazole-3-carboxaldehyde **3** (1.8 mmol, 452.3 mg) was used instead. The target compound was obtained in 21.2% yield (318.5 mg). UV-vis (CH_2Cl_2), λ_{max} / nm (log ε): 414 (5.16). ^{1}H NMR ($CDCl_3$, 600 MHz) δ_H 9.13 (d, *J* = 6 Hz, 2H), 8.89 (d, *J* = 2.4 Hz, 1H), 8.75 (d, *J* = 6 Hz, 4H), 8.69-8.68 (m, 2H), 8.29−8.18 (m, 2H), 7.76(s, 1H),7.59−7.57 (m, 2H), 7.31(s, 1H), 4.56 (t, *J* = 1.2*,* 2H), 2.08-2.12 (m, 2H), 1.61-1.63(m, 2H), 1.10 (t, *J* = 4.8*,* 3H) ppm. High-resolution ESI-MS (negative): *m/z* = 850.2023 (Calcd for $C_{47}H_{26}F_{10}N_5$ $[M-H]^-$ = 850.2014). 9.13, 8.89, 8.74, 8.70, 8.58, 8.28, 8.19, 7.59,

1.2.4 Synthesis of Ga^{III}triarylcorrole G-2. The general synthetic procedure is similar to that of **G-1** except H_3triarylcorrole **C-2** (85.17 mg, 0.1 mmol) was used instead. The target compound was obtained in 60.1% yield (55.1 mg). UV-vis (CH_2Cl_2), λ_{max} / nm (log ε): 425 (4.74). ^{1}H NMR ($CDCl_3$, 600 MHz) δ_H 9.23 (d, *J* = 6 Hz, 2H), 8.86 (d, *J* = 6 Hz, 2H), 8.85 (s, 1H), 8.83 (d, *J* = 6 Hz, 1H), 8.81 (d, *J* = 4.2 Hz, 4H), 8.79(d, *J* = 4.2 Hz, 2H), 8.21-8.19 (m, 1H), 8.13 (d, *J* = 7.8 Hz, 2H), 7.70 (d, *J* = 7.8 Hz, 2H), 7.54-7.58 (m, 2H), 7.24-7.25 (s, 1H), 6.67 (t, *J* = 7.8 Hz, 2H), 5.88 (t, *J* = 7.2 Hz, 2H), 4.54 (t, *J* = 7.2 Hz, 2H), 2.98 (d, *J* = 5.4 Hz, 2H), 2.08 (t, *J* = 7.2 Hz, 2H), 1.57-1.62 (m, 2H), 1.08 (t, *J* = 7.2 Hz, 3H), ppm. High-resolution ESI-MS (negative): *m/z* = 996.1608 (Calcd for $C_{52}H_{30}F_{10}GaN_6$ $[M]^-$ = 996.1608). Elemental analysis: Calcd. for $C_{52}H_{29}F_{10}GaN_6$, C, 62.61; H, 2.93; N, 8.42; Found, C, 62.87; H, 3.06; N, 8.33.

1.2.5 Synthesis of quaternized Ga^{III}triarylcorrole G-2Q. Ga^{III}triarylcorrole **G-2** (32 mg, 0.032 mmol) and iodoethane (0.1 mL, 12 mmol) were dissolved in 10 mL dry DMF, stirred and refluxed at 60°C for 24 h under N_2 in the absence of light. The reaction mixture was cooled, and cold diethyl ether was added to precipitate out **G-2Q**. The precipitate was

filtered and washed with diethyl ether and dried to afford the target compound 78% yield (25.0 mg). UV-vis (CH_2Cl_2), λ_{max} / nm (log ε): 424 (4.72). ^{1}H NMR $(CD_3)_2CO$, 600 MHz) δ 9.34 (d, *J* = 3.9 Hz, 2H), 9.04 (d, *J* = 4.3 Hz, 2H), 8.97 (d, *J* = 3.5 Hz, 2H), 8.92 (s, 1H), 8.85 (d, *J* = 4.4 Hz, 2H), 8.27 (t, *J* = 7.4 Hz, 2H), 7.94 (d, *J* = 8.2 Hz, 1H), 7.73 (d, *J* = 8.5 Hz, 2H), 7.55 (t, *J* = 7.8 Hz, 1H), 7.24 (t, *J* = 7.3 Hz, 2H), 7.05 (s, 1H), 6.29 (s, 2H), 4.68 (t, *J* = 7.1 Hz, 2H), 3.44 (s, 2H), 1.62 (dd, *J* = 15.2, 7.5 Hz, 3H), 1.42 (s, 1H), 1.29 (d, *J* = 9.9 Hz, 1H), 1.20 (s, 2H), 1.07 (t, *J* = 7.4 Hz, 3H) ppm. MS (MALDI-TOF-MS): *m/z* = 1027.12 (Calcd for $C_{54}H_{36}F_{10}GaN_6$ $[M+H]^+$ = 1027.20). Elemental analysis: Calcd. for $C_{54}H_{34}F_{10}GaN_6$, C, 63.18; H, 3.34; N, 8.19; Found, C, 63.35; H, 3.48; N, 8.05.

1.3 PDT activity studies

The MCF-7 cancer cell line was used in the dark toxicity and photodynamic activity studies. It was cultured to 100% confluence and seeded to a 96-well plate following a previously described literature protocol [S1]. Stock solutions were prepared for **G-1**, **G-2** and **G-2Q** in DMSO. Drug aliquots for cell studies were then prepared in PBS media with < 1% DMSO after dilution and administered over a gradient concentration range of 0.7−50 μM. Irradiations were performed at 595 nm for 20 min using a Thorlabs M595L3 light-emitting diode (LED) mounted onto the housing of a Modulight 7710-680 medical laser system. An irradiance value of 250 mW.cm^{-2} was determined with a Coherent FieldmaxII TOP energy/power meter and Powermax PM10 sensor. Percentage cell viabilities were determined on a Synergy 2 multi-mode microplate reader (BioTek®) at 540 nm using the MTT assay [S2]. The experiments were performed in triplicate, and the data were analyzed by using ANOVA and student T-test. The percentage cell viability values were determined in a manner described previously in the literature from the ratio of the absorbance of the active cells after the treatments involving the photosensitizer dye and the absorbance of the control cells in 1% DMSO culture media [S1]. Error bars provide the standard deviation (n = 3).

1.4 Cellular uptake

Cellular uptake studies were carried out with the MCF-7 cell line for **G-1**, **G-2** and **G-2Q**

using a previously described literature procedure [S3]. *Ca.* 10^4 cells were seeded on a 96-well plate. 10 μM **G-1**, **G-2** and **G-2Q** was added, and the cells were incubated for 24 h, since it has recently been reported in the literature for similar Ga^{III}triarylcorrole complexes that optimal cellular uptake was observed after 24 h [S4]. After 24 h of treatment with **G-1**, **G-2** or **G-2Q**, the cells were washed three times with 100 μL DPBS to remove any residual dye. Cellular uptake in the treated MCF-7 cells was quantified at the emission band maximum of each dye on a Synergy 2 multi-diode microplate reader (BioTek) by determining the fluorescence intensity.

1.5 Lipophilicity studies

Lipophilicity is an important parameter for determining the ability of photosensitizer dyes to bioaccumulate [S5, S6]. The lipophilicities of **G-1**, **G-2** and **G-2Q** were determined in triplicate with the "shake-flask" approach [S7]. 0.5 mg of each Ga^{III}triarylcorrole was dissolved in dry $CHCl_3$ (10 mL), and the absorbance value at the B band maximum was determined with 3 mL of each solution (A_o). 3 mL of ultrapure water was added, and the mixtures were stirred at room temperature for 4 h and then centrifuged for 10 min at 5000 rpm to separate the $CHCl_3$ and water phases. The absorbance value of the $CHCl_3$ layer was recorded at the B band maximum (A_{final}). The absorbance value in water (A_w) was calculated from this, $A_w = A_o - A_{final}$, so that partition coefficients (log $P_{o/w}$) could be determined on the basis of log (A_o / A_w) by using Equation 1 [S7] and the partition coefficients of the complexes between $CHCl_3$:H_2O (Log $P_{chloroform}$).

$$P_{octanol} = [1.343 + \text{Log } P_{chloroform}] / 1.126 \quad (1)$$

1.6 Antimicrobial studies

1.6.1 Planktonic bacteria

The bacteria culture was grown according to literature procedures to achieve a concentration of *ca.* 10^8 CFU.mL^{-1} for the studies on planktonic bacteria [S8]. The manufacturer's specifications were followed to obtain an individual colony on an agar plate. The colony was inoculated into 5 mL of fresh nutrient broth and kept overnight at 37°C on a rotary shaker (*ca.* 200 rpm). Aliquots (100 μL) were regularly taken from the bacteria culture

suspension to measure the optical densities using a Ledetect 96 (Labxim Products) so that a mid-logarithmic phase (OD 620 nm ≈ 0.6) was ultimately obtained. The bacterial culture was harvested by centrifuging at 3000 rpm for 15 min to remove the broth, and the bacteria pellets were washed in PBS three times and resuspended in 4 mL PBS. A working stock solution for the studies involving planktonic bacteria was obtained through a further dilution by a factor of 10^3 in PBS.

Stock solutions of **G-1**, **G-2** and **G-2Q** were prepared in PBS. 5 mL aliquots of the stock solutions, and either *S. aureus* or *E. coli* were prepared to provide the final concentrations for study of 0.5 and 2.5 μM against *S. aureus* and 10 μM against *E. coli*. The mixtures were incubated for 30 min at 37°C in the dark in an oven fitted with a shaker. 2.5 mL of these solutions were illuminated in a 24 well plate with a Thorlabs M595L3 595 nm LED mounted onto the housing of a Modulight 7710-680 medical laser system (250 $mW.cm^{-2}$), while the other 2.5 mL was kept on a second plate in the dark as a control. After 15, 30, 60, 90, 120 min irradiation time for *S. aureus* and *E. coli* suspensions treated with 0.5 and 10 μM of dye and 5, 15, 30, 45, 60, 75 min for *S. aureus* suspensions treated with 2.5 μM of the dyes, a 100 μL sample was spotted onto agar plates by micropipette. The plates were then incubated for 24 h at 37°C in the dark. A Scan 500 Automatic Colony Counter (Healthcare Technologies) was used to calculate $CFU.mL^{-1}$ values. Survival fractions were determined by comparison with a control solution that contained no Ga^{III}triarylcorrole dye. Triplicate experiments were carried out to enable the calculation of standard deviations.

Prior to the time-dependent studies, concentrations studies were also carried out to establish the optimal concentrations of Ga^{III}triarylcorroles for the photoinactivation studies with *S. aureus* and *E. coli* by following the same procedure. For concentration studies, 0.5, 1, 2, 2.5, and 5 μM of Ga^{III}triarylcorroles were used against *S. aureus*, and 2.5, 5, 10, 15, and 20 μM against *E. coli* and irradiations were carried out by using Thorlabs M595L3 LED (250 $mW.cm^{-2}$) for 60 min in the manner described above.

1.6.2 Biofilm bacteria

The single species *S. aureus* and *E. coli* biofilm bacteria were grown in sterilized 96-

well plates following previously described methods [S9-S11] using freshly prepared bacteria culture solutions (10^6 CFU.mL^{-1}) in tryptic soy broth (TBS). 200 µL.well^{-1} of these TBS supplemented bacteria cultures were seeded into the 96-well plates and incubated anaerobically under static conditions at 37 °C under a 5% CO_2 atmosphere for 24 and 72 h for *S. aureus* and *E. coli*, respectively. Wells with TBS media alone served as negative controls to quantify the biofilm growth. After incubation, the culture media was gently discarded, followed by rinsing the wells two times with PBS to remove the residual nutrient broth and unattached planktonic bacteria cells. The plates were air-dried at room temperature for 30 min to fix the attached cells. The biofilm bacteria growth was measured using the crystal violet assay. The biofilm-coated wells were stained with a 150 µL.well^{-1} aliquot of 0.1% (*w/v*) crystal violet assay for 15 min at room temperature. After 15 min, the crystal violet solution was discarded, and the wells were rinsed three times using PBS (200 µL.well^{-1}) to remove the excess dye. 150 µL.well^{-1} of PBS was once again added to the stained wells, and the absorbances of the well solutions were measured at 590 nm on a Synergy 2 multi-mode microplate reader (BioTek®). All the experiments were carried out in three independent triplicates. Outlier values were identified using the Z-score method, and the non-outlier values were used to calculate the average biofilm formed. From the biofilms absorbance data, the average negative control value was subtracted. The data is provided as mean absorbance ± standard deviation. When the absorbance value at 590 nm was three times the standard deviation of the negative control mean absorbance, the biofilms were considered to be fully formed [S11].

Viable cell counts of the single species *S. aureus* and *E. coli* biofilms were also determined using the viable colony count method. This was done by dissolving the biofilms formed in the 96-well plates with 200 µL.well^{-1} of PBS. The plates were sonicated vigorously for 10 min, and the wells were gently scraped to remove the attached cells. The resultant well contents were vortexed to homogenize the suspension and serially diluted ten-fold. A 100 µL aliquot of the diluted sample was aseptically inoculated on the agar plate and incubated at 37 °C for 24 h. After 24 h incubation, viable colonies were counted (CFU.mL^{-1}) on a Scan 500® series Automatic Colony Counter. All the experimental data were analyzed statistically using student T-test and ANOVA.

For *in vitro* dark and light studies for Ga^{III}triarylcorroles against the single-species biofilms of *S. aureus* and *E. coli* strains, concentration studies were carried out prior to time-dependent studies. During the concentration studies, the 96-well plates were coated with *S. aureus* and *E. coli* strains and grown and rinsed as described above. The bacteria were incubated with 100 μLwell^{-1} aliquots of Ga^{III}triarylcorroles in PBS at 15, 30, 60, 120 and 240 μM concentrations for 30 min. After incubation, the biofilm coated wells were irradiated for 30 min using a Thorlabs LED M595L3 (250 mW.cm^{-2}) in the manner described above to assess the phototoxicities of the dyes. At the same time, similar samples were kept in the dark for the same period of time to determine the dark cytotoxicity values. The wells with PBS media alone (untreated biofilms) served as the control. After the dark and light treatments, the supernatant liquid was discarded, and the wells were gently rinsed with PBS. The crystal violet assay (150 μL.well^{-1}) was used to quantify the biofilm cells densities, and the absorbance of the well solutions was measured at 590 nm on a Synergy 2 multi-mode microplate reader (BioTek®) and directly using the viable colony count method as previously described.

The experimental procedure for time-dependent studies was the same as the one used for the concentration studies, with fixed concentrations of the dyes used at different irradiation time intervals. Both dark and light studies were carried out. For these studies, 30 and 60 μM of Ga^{III}triarylcorroles were used to treat the single species *S. aureus* and *E. coli* biofilm bacteria, respectively, and the photo-irradiations were carried out at 15, 30, 60, 90, 120 min time intervals using a Thorlabs LED M595L3 (250 mW.cm^{-2}) in in the manner described above. Crystal violet assay and viable colonies count methods were used to quantify the biofilm cell densities and carry out a comparison with the controls as previously described. All the experiments were performed in three independent triplicates, and data were analyzed statistically using student T-test and ANOVA.

1.7 Photostability. The photostability of **G-1**, **G-2** and **G-2Q** was studied in 1% DMSO/H_2O solutions irradiated at 595 nm using a Thorlabs M595L3 LED (250 mW.cm^{-2}) for 30 min under the same conditions used for the MCF-7 cell studies and antimicrobial experiments with *S. aureus* and *E. coli*. The experimental progress was monitored at 15 min intervals on

a Shimadzu UV-2550 spectrophotometer by recording the absorbance value of the B band maximum.

1.8 Photophysical parameters. Comparative methods were used to determine the fluorescence (Φ_F) and singlet oxygen (Φ_Δ) quantum yield values for **G-1**, **G-2** and **G-2Q** in DMSO. ZnTPP (Φ_F = 0.0397) was used as the standard for the fluorescence measurements [S12]. To determine the Φ_Δ values, 1,3-diphenylisobenzofuran (DPBF) was used as a singlet oxygen quencher, while Rose Bengal was used as the standard (Φ_Δ = 0.76) [S13].

1.9 Theoretical calculations. The geometries of **G-1** and **G-2** and an A_3 symmetry Ga^{III}-tri-pentafluorophenylcorrole (**G-F**) and Ga^{III}triphenylcorrole (**G-H**) model complexes were optimized using the B3LYP functional with the default SDD basis sets of the Gaussian 09 software packages [S14]. The optimized B3LYP geometries were then used to carry out TD-DFT calculations using the CAM-B3LYP functional, since it has a long-range correction and is better suited for predicting the relative energies of excited states with significant intramolecular charge transfer character. The *t*-butyl and *n*-butyl groups of **G-1** and **G-2** were replaced with methyls to simplify the calculations.

2. Tables

Table S1. Solvent dependence of the B band λ_{max} values of **G-1** and **G-2**.

Solvent	Acetone	Benzene	Toluene	DMSO	MeCN	DMF	CH_2Cl_2	THF	Hexane	MeOH
λ_{max}**G-1**	422	425	425	426	421	425	422	422	419	422
λ_{max}**G-2**	420	423	424	424	420	424	422	422	420	422
n	1.632	1.501	1.497	1.477	1.432	1.431	1.424	1.401	1.375	1.328
ε	20.7	2.28	2.4	47.24	37.5	38.25	8.93	7.58	1.9	32.7
f(n)	0.182	0.227	0.226	0.22	0.175	0.205	0.203	0.198	0.186	0.169
f (n, ε)	0.646	-	-	0.657	0.665	0.667	-	-	-	0.71

Table S2. The fluorescence emission data for Ga^{III}triarylcorrole **G-1** in various solvents (λ_{ex} = 410 nm).

	λ_{em} (nm)	Solvent	Φ_F (%)	τ_f [ns]
	609, 636	Toluene	10.13	2.24
	610, 662	THF	12.60	2.71
G-1	610, 668	CH_2Cl_2	9.22	2.06
	616, 674	MeOH	8.42	2.35
	619, 677	MeCN	7.57	2.01
	612, 644	Toluene	9.57	2.05
	613, 669	THF	10.82	2.49
G-2	615, 672	CH_2Cl_2	8.09	1.78
	620, 682	MeOH	7.36	2.18
	623, 680	MeCN	7.57	1.92

Table S3. The transient-state fluorescence data of **C-1**, **C-2**, **G-1** and **G-2** in CH_2Cl_2 (λ_{ex} = 410 nm).

	λ_{em} (nm)	Φ_F (%)	τ_f [ns]	K_{nr} [10^8 s^{-1}]	K_r [10^8 s^{-1}]
C-1	657	7.08	3.78	0.246	0.0187
C-2	662	8.56	3.63	0.252	0.0236
G-1	609	9.22	2.06	0.441	0.0447
G-2	616	10.39	1.86	0.482	0.0559

Table S4. Photophysicochemical properties of **G-1**, **G-2** and **G-2Q** in DMSO.

	λ_{Abs} (nm)		λ_{em} (nm)	Φ_F	τ_F (ns)	τ_T (μs)[a]	Φ_Δ
	B	Q		± 0.02	± 0.01	± 0.01	± 0.01
G-1	423	574, 604	630, 694	0.071	1.63	255 (32.6)	0.66
G-2	422	573, 602	629, 691	0.073	1.54	193 (47.5)	0.67
G-2Q	424	578, 600	630, 688	0.062	1.74	42.4 (26.3)	0.64

a - Triplet lifetimes under nitrogen gas and in bracket are for the samples in an oxygen environment (i.e. unpurged solutions).

Table S5. Water partition coefficient values (Log $P_{o/w}$) of **G-1**, **G-2** and **G-2Q**.

	Log $P_{o/w}$ (± 0.01)
G-1	1.74
G-2	1.44
G-2Q	1.01

Table S6. IC_{50} and phototoxicity index (PI) values for **G-1**, **G-2** and **G-2Q** against MCF-7 cancer cell line and their photostabilities in 1% DMSO:H_2O solutions.

	IC_{50} (μM) dark	**IC_{50} (μM) light**	**PI (dark/light)**	**Photostability (%)**
G-1	> 50	24.8 (±1.2)	> 2.01	92
G-2	> 50	16.2 (±1.1)	> 3.09	94
G-2Q	> 50	7.8 (±0.6)	> 6.45	91

Table S7. Log reduction values for **G-1**, **G-2** and **G-2Q** in 1% DMSO/PBS against planktonic *S. aureus* and *E. coli*.

	S. aureus				***E. coli***	
	Conc. (μM)	**Log reduction**	**Conc. (μM)**	**Log reduction**	**Conc. (μM)**	**Log reduction**
G-1	0.5	2.79	2.5	3.66	10	2.40
G-2	0.5	3.23	2.5	7.78	10	2.65
G-2Q	0.5	7.78	2.5	7.78	10	3.26

Table S8. Log reduction and cell viability values for **G-1**, **G-2** and **G-2Q** against biofilm cells of *S. aureus* and *E. coli* in 1% DMSO/PBS after 120 min of illumination at 595 nm with a Thorlabs M595L3 LED (250 $mW.cm^{-2}$).

	S. aureus			***E. coli***		
	Conc. (μM)	**Log reduction**	**Cell Viability (%)**	**Conc. (μM)**	**Log reduction**	**Cell Viability (%)**
G-1	30	1.22	6.0	60	0.65	22.2
G-2	30	1.27	5.4	60	0.71	19.6
G-2Q	30	2.02	0.9	60	1.10	8.2

Table S9 Calculated UV-vis absorption spectra of B3LYP optimized geometry of parent **G-F**, **G-1**, **G-2** and **G-H** obtained by using the CAM-B3LYP functional with SDD basis sets.

G-F							
Band[a]	**#[b]**	**Calc[c]**			**Exp[d]**		**Wave Function[e] =**
----	1	----	----	----	----	----	Ground State
Q	2	18.9	530	(0.11)	-	-	**70% s** → **-a; 28% a** → **-s;** …
	3	19.8	505	(0.02)			**64% a** → **-a; 33% s** → **-s;** …
-	4	25.9	386	(0.05)	-	-	84% s → L+2[py]; **10% s** → **-s;** …
-	5	27.5	363	(0.45)	-	-	47% a → L+2[py]; **35% a** → **-s; 10% s** → **-a;** …
B	6	27.8	359	(0.87)	-	-	**46% s** → **-s; 25% a** → **-a;** 17% a → L+2[py]; …
	7	28.2	354	(0.89)			34% a → L+2[py]; **32% a** → **-s; 17% s** → **-a;** …
G-1							
Band[a]	**#[b]**	**Calc[c]**			**Exp[d]**		**Wave Function[e] =**
----	1	----	----	----	----	----	Ground State
Q	2	18.5	541	(0.18)	16.6	604	**75% s** → **-a; 15% a** → **-s;** …
	3	19.5	512	(0.02)	17.4	574	**64% a** → **-a; 24% s** → **-s;** …
-	4	24.3	412	(0.02)	-	-	52% s → L+2[py]; **43% s** → **-s;** …
-	5	26.8	373	(0.07)	-	-	**55% a** → **-s;** 43% a → L+2[py]; …
B	6	27.6	363	(1.34)	23.6	423	34% a → L+2[py]; **31% s** → **-s; 31% a** → **-a;** …
	7	28.3	354	(1.03)			47% a → L+2[py]; **27% a** → **-s; 21% s** → **-a;** …
G-2							
Band[a]	**#[b]**	**Calc[c]**			**Exp[d]**		**Wave Function[e] =**
----	1	----	----	----	----	----	Ground State
Q	2	18.4	543	(0.19)	16.6	602	**78% s** → **-a; 10% a** → **-s;** 10% a → L+1[py]; …
	3	19.5	514	(0.03)	17.5	573	**65% a** → **-a;** 19% s → L+1[py]; **14% s** → **-s;** …
-	4	24.0	416	(0.03)	-	-	63% s → L+1[py]; **31% s** → **-s;** …
-	5	26.4	378	(0.13)	-	-	83% a → L+1[py]; **12% a** → **-s;** …
B	6	27.8	360	(1.28)	23.7	422	**53% s** → **-s; 30% a** → **-a;** 16% s → L+1[py]; …

	7	28.5	351	(0.91)			**78% a → -s; 18% s → -a;** …
G-H							
Band[a]	**#[b]**	**Calc[c]**			**Exp[d]**		**Wave Function[e] =**
----	1	----	----	----	----	----	Ground State
Q	2	18.4	542	(0.21)	-	-	**79% s → -a; 18% a → -s;** …
	3	20.0	500	(0.00)			**49% a → -a; 31% s → -s;** 18% s → L+1^{py}; …
-	4	21.1	473	(0.01)	-	-	80% s → L+1^{py}; **10% s → -s;** …
-	5	24.8	403	(0.02)	-	-	96% a → L+1^{py}; …
-	6	26.7	374	(0.00)	-	-	99% s → L+3^{py}; …
B	7	27.8	360	(1.13)	-	-	**58% s → -s; 39% a → -a;** …
	8	28.7	349	(1.15)			**76% a → -s; 20% s → -a;** …

[a] The assignment of the bands is described in the main text.[b] States predicted in the TD-DFT calculations are numbered in ascending energy terms. [c] Calculated band energies (10^3.cm^{-1}) and wavelengths (nm) with the oscillator strength values in parentheses (f). [d] Observed energies (10^3.cm^{-1}) and wavelengths (nm) in DMSO from Table 4. [e] The wave functions calculated from the eigenvectors in the TD-DFT calculations. Bold face highlights the one-electron transitions between the **a**, **s**, **-a** and **-s** MOs. Only contributions > 10% are shown.

3. Mass spectra

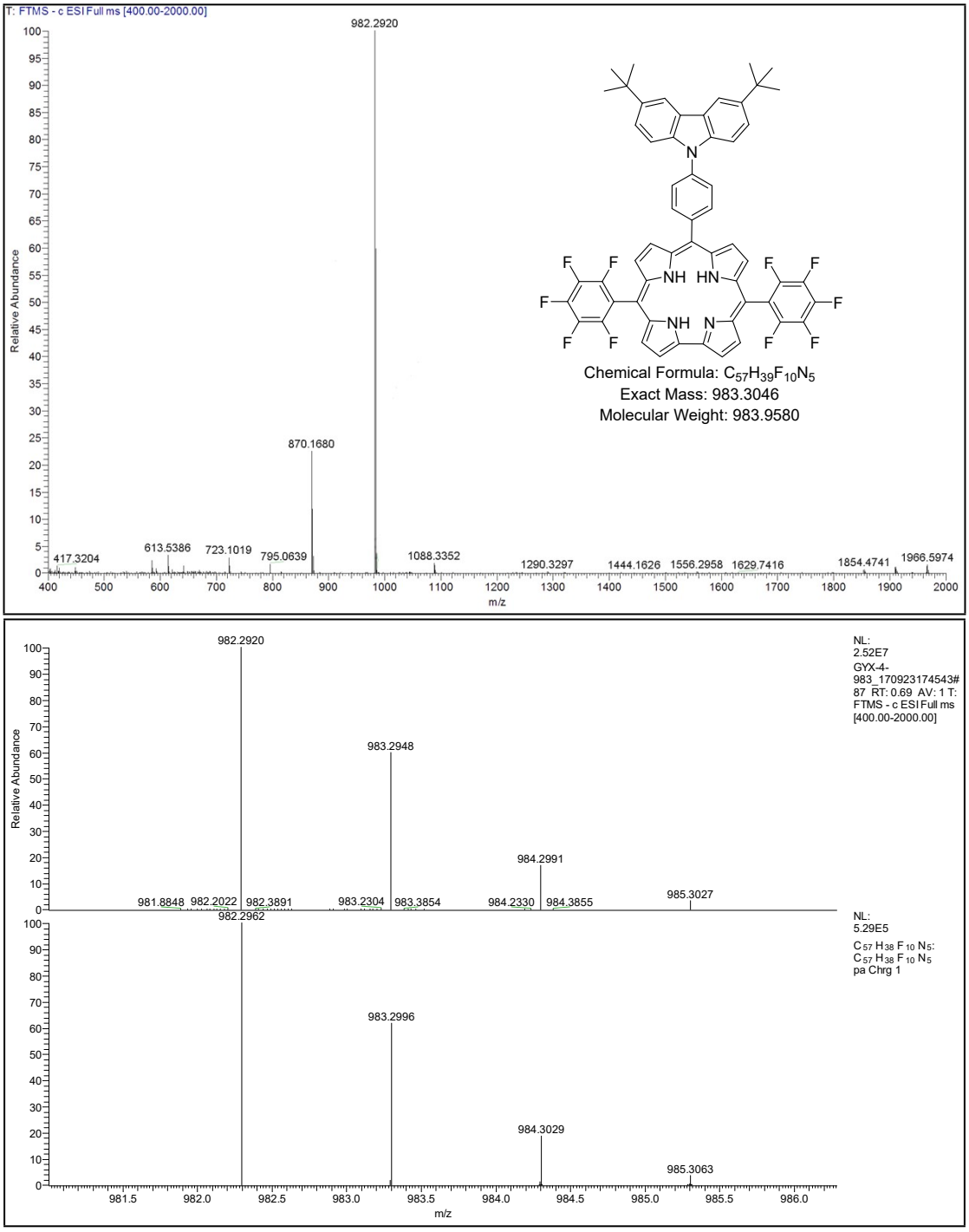

Figure S1. ESI-High-resolution mass spectrometry data for **C-1** in negative ion mode.

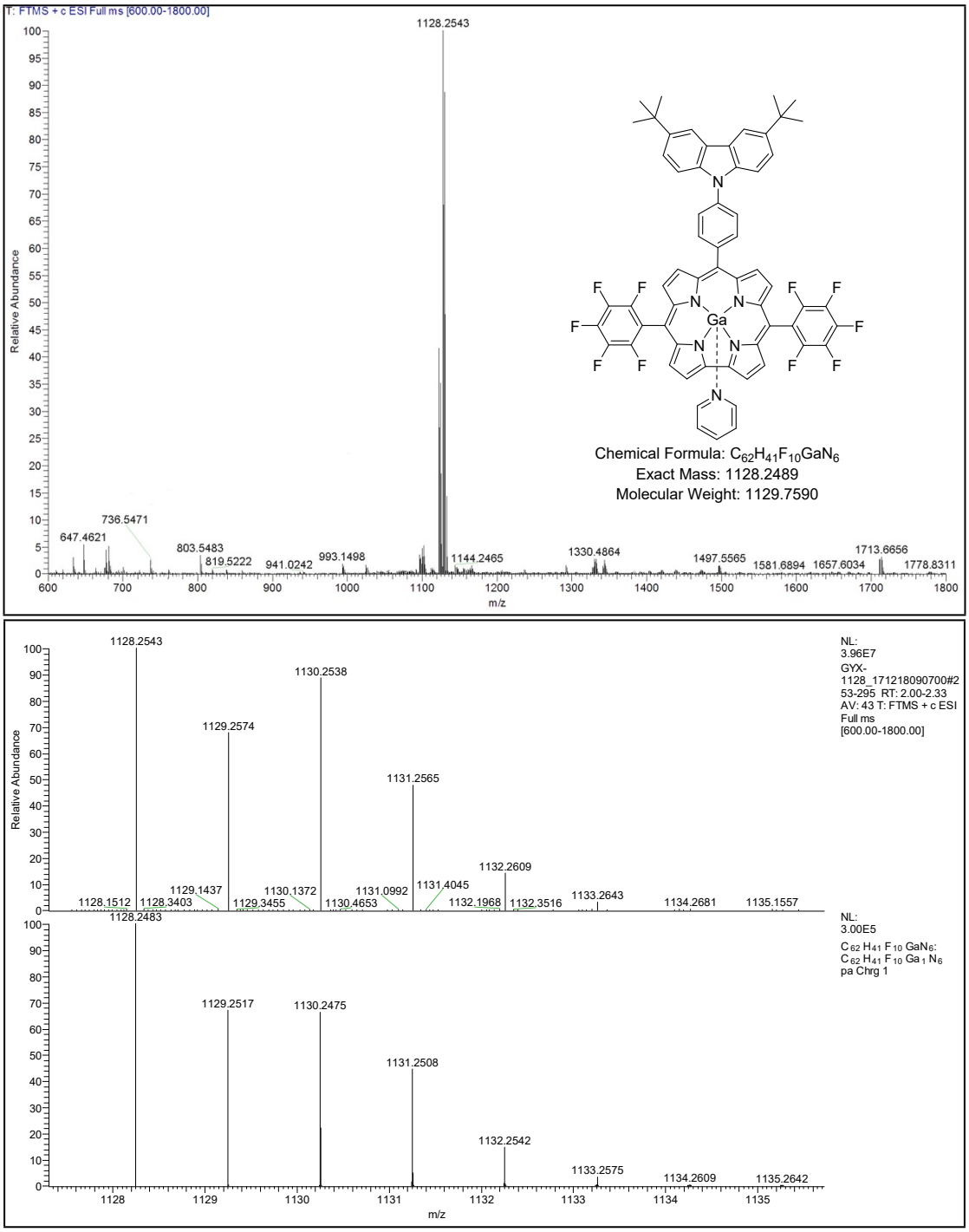

Figure S2. ESI-High-resolution mass spectrometry data for **G-1** in negative ion mode.

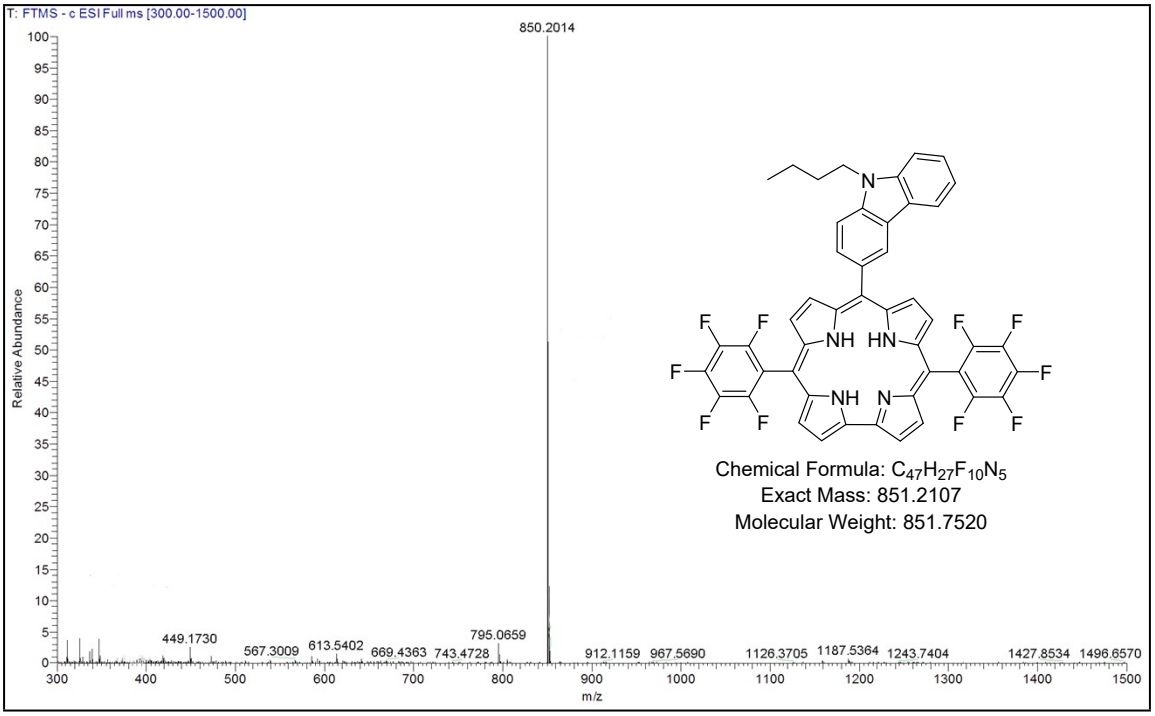

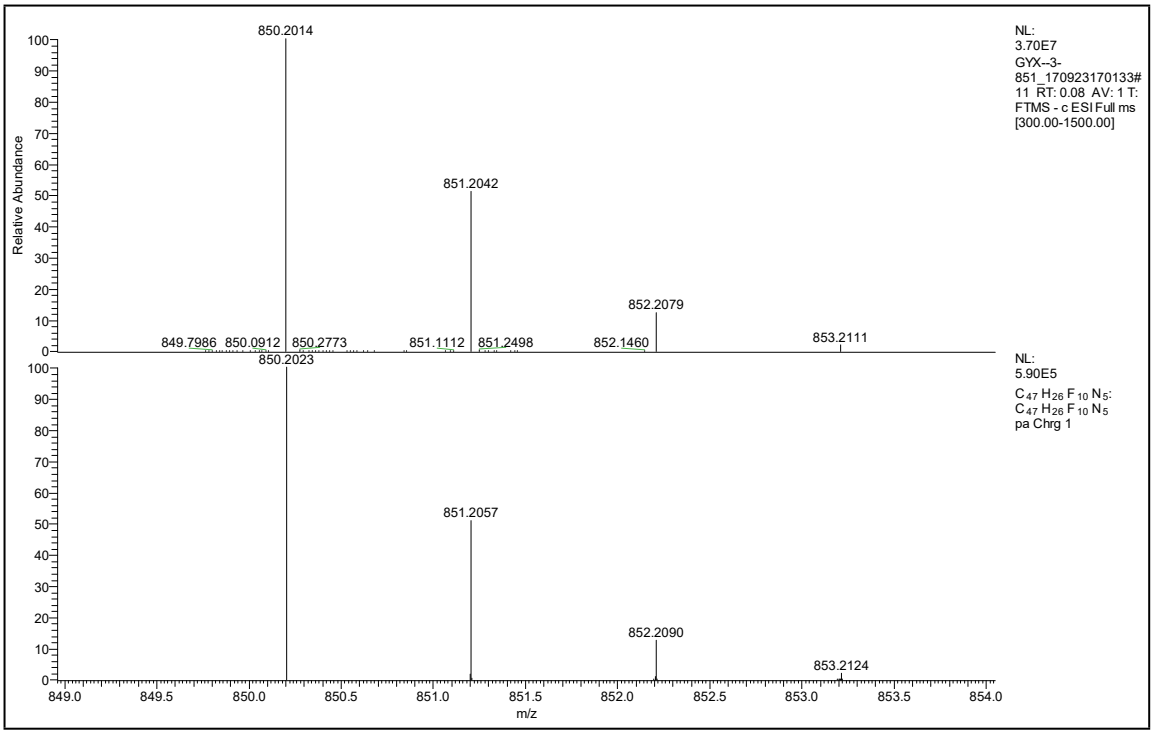

Figure S3. ESI-High-resolution mass spectrometry data for **C-2** in negative ion mode.

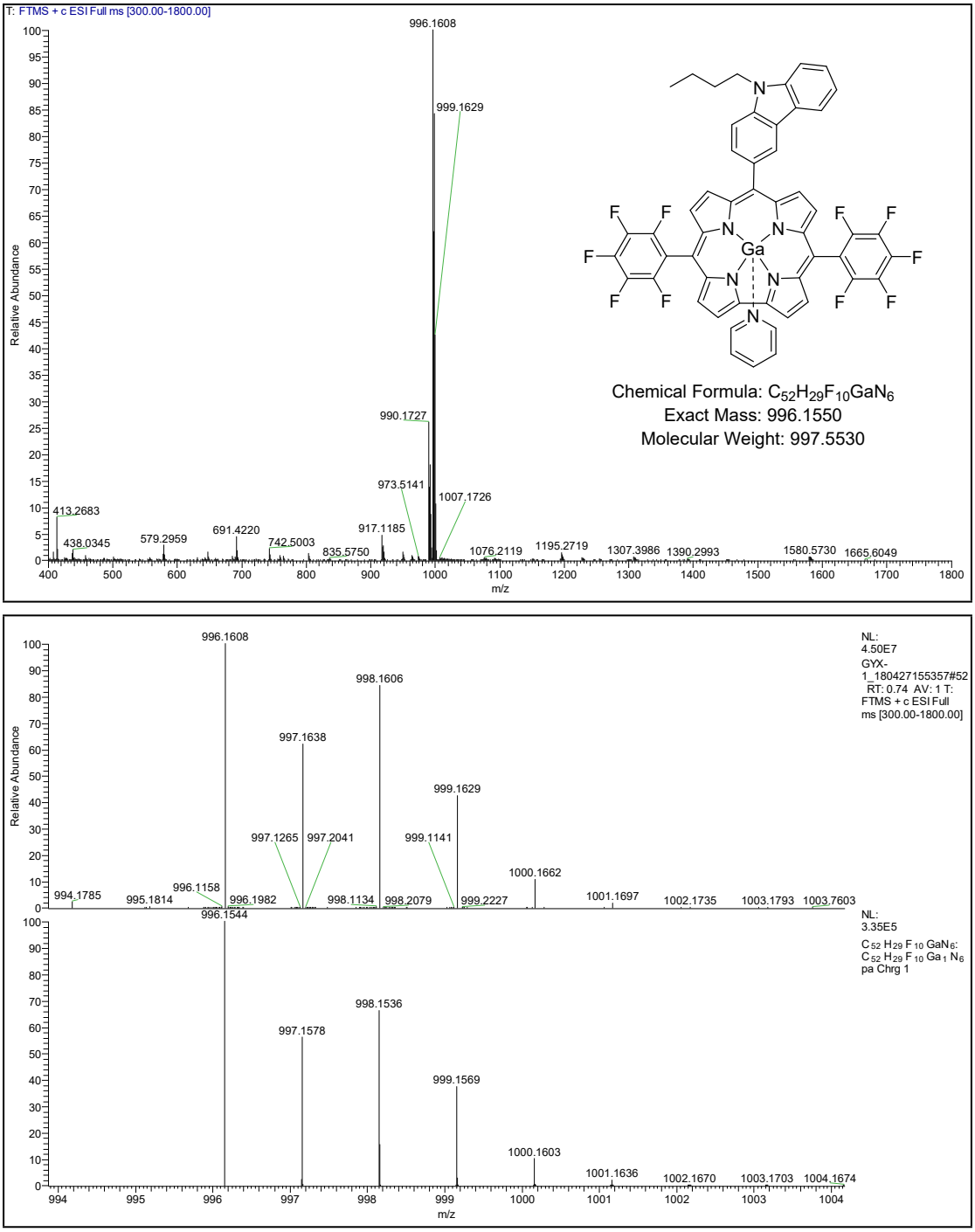

Figure S4. ESI-High-resolution mass spectrometry data for **G-2** in negative ion mode.

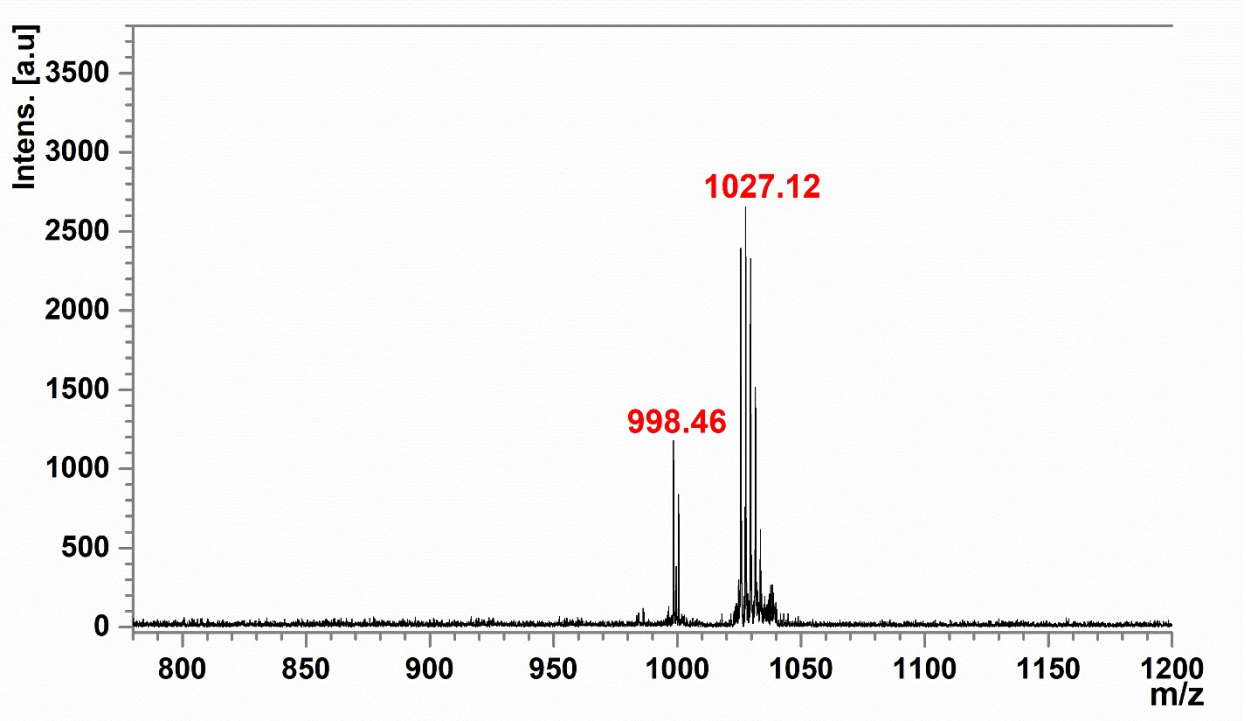

Figure S5. MALDI-TOF MS data for **G-2Q**.

4. ^{1}H NMR spectra

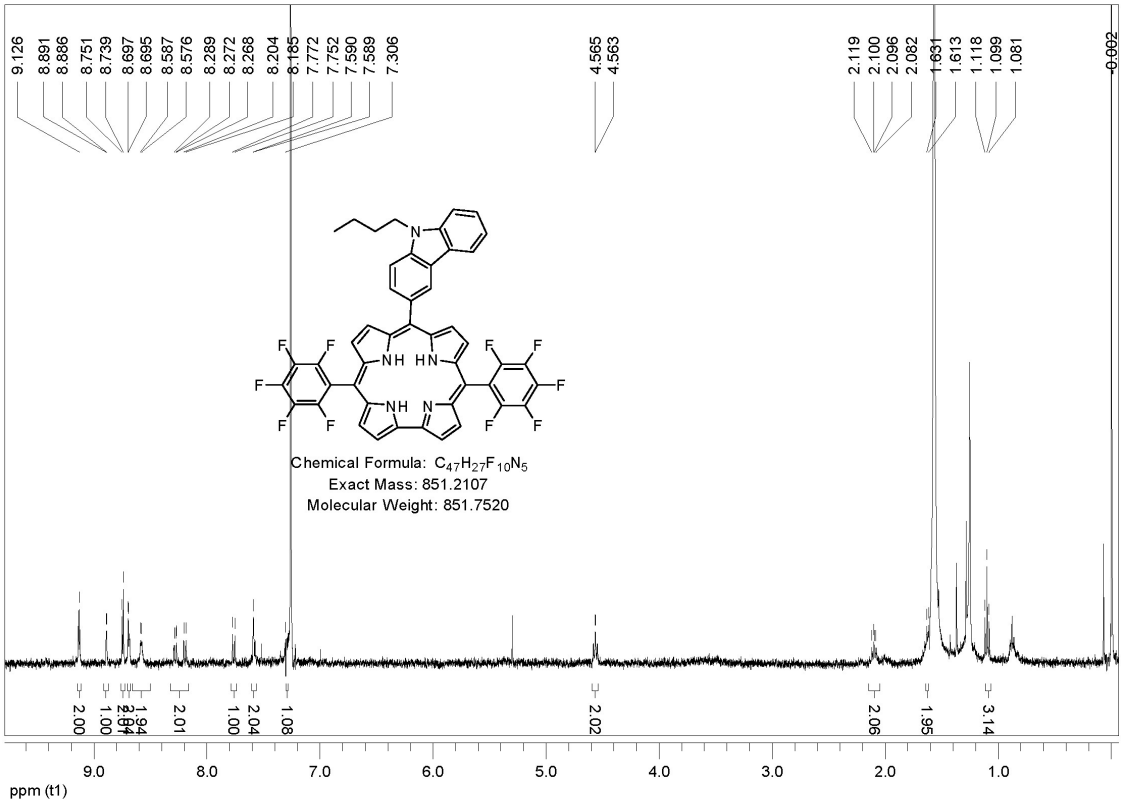

Figure S6. ^{1}H NMR spectrum of **C-2** in ($CDCl_3$, 600 M).

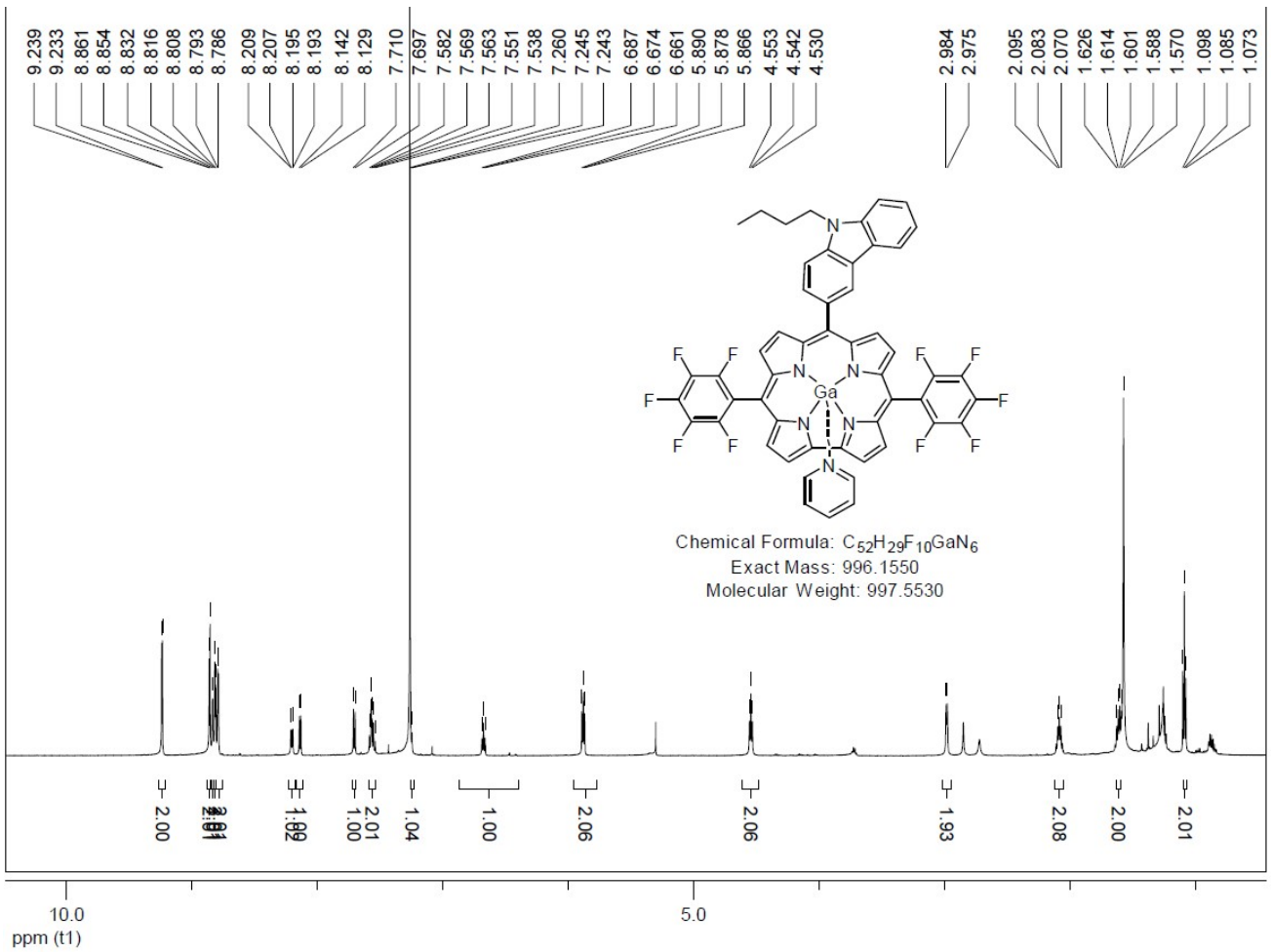

Figure S7. ^{1}H NMR spectrum of **G-2** ($CDCl_3$, 600 M).

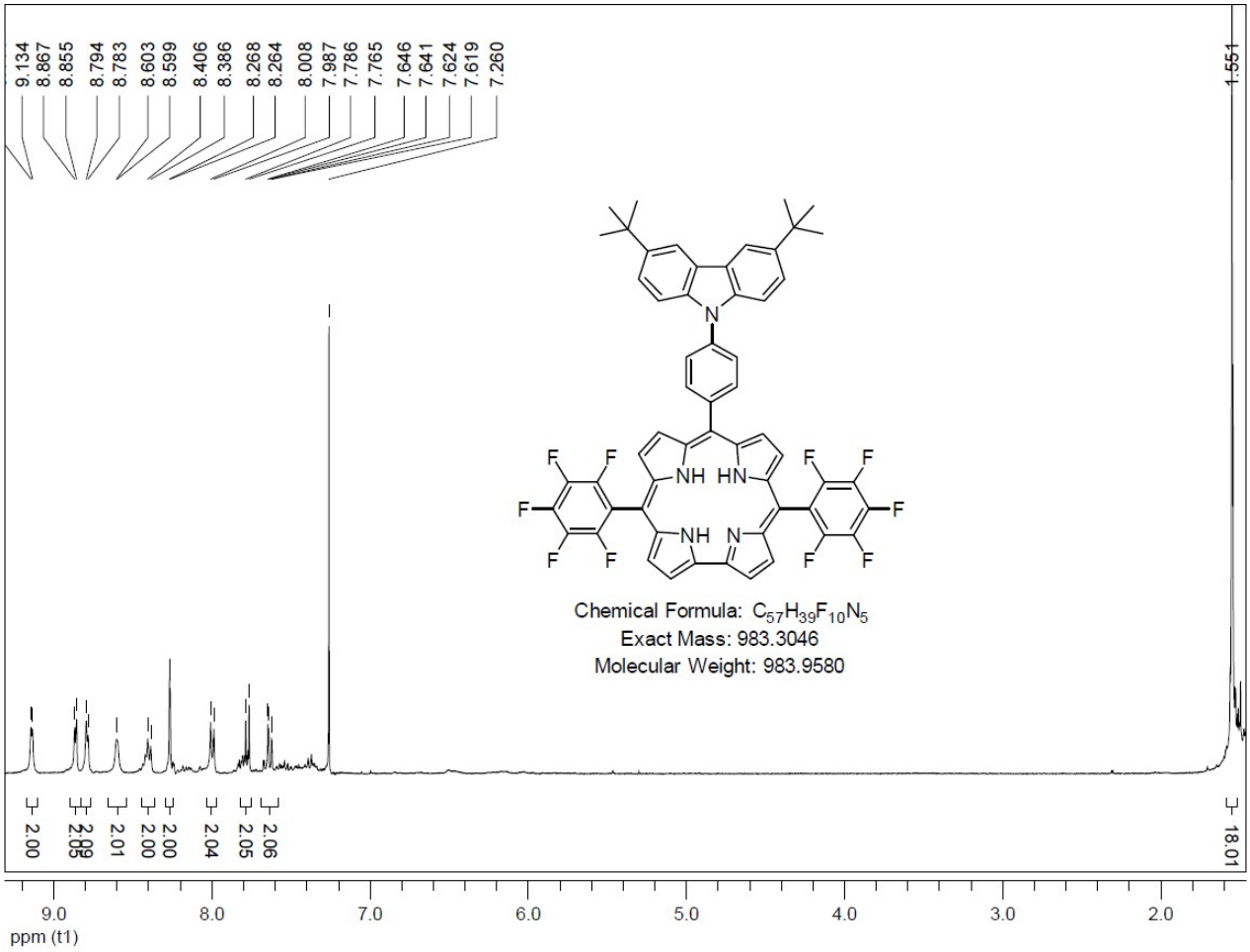

Figure S8. ^{1}H NMR spectrum of **C-1** ($CDCl_3$, 600 M)

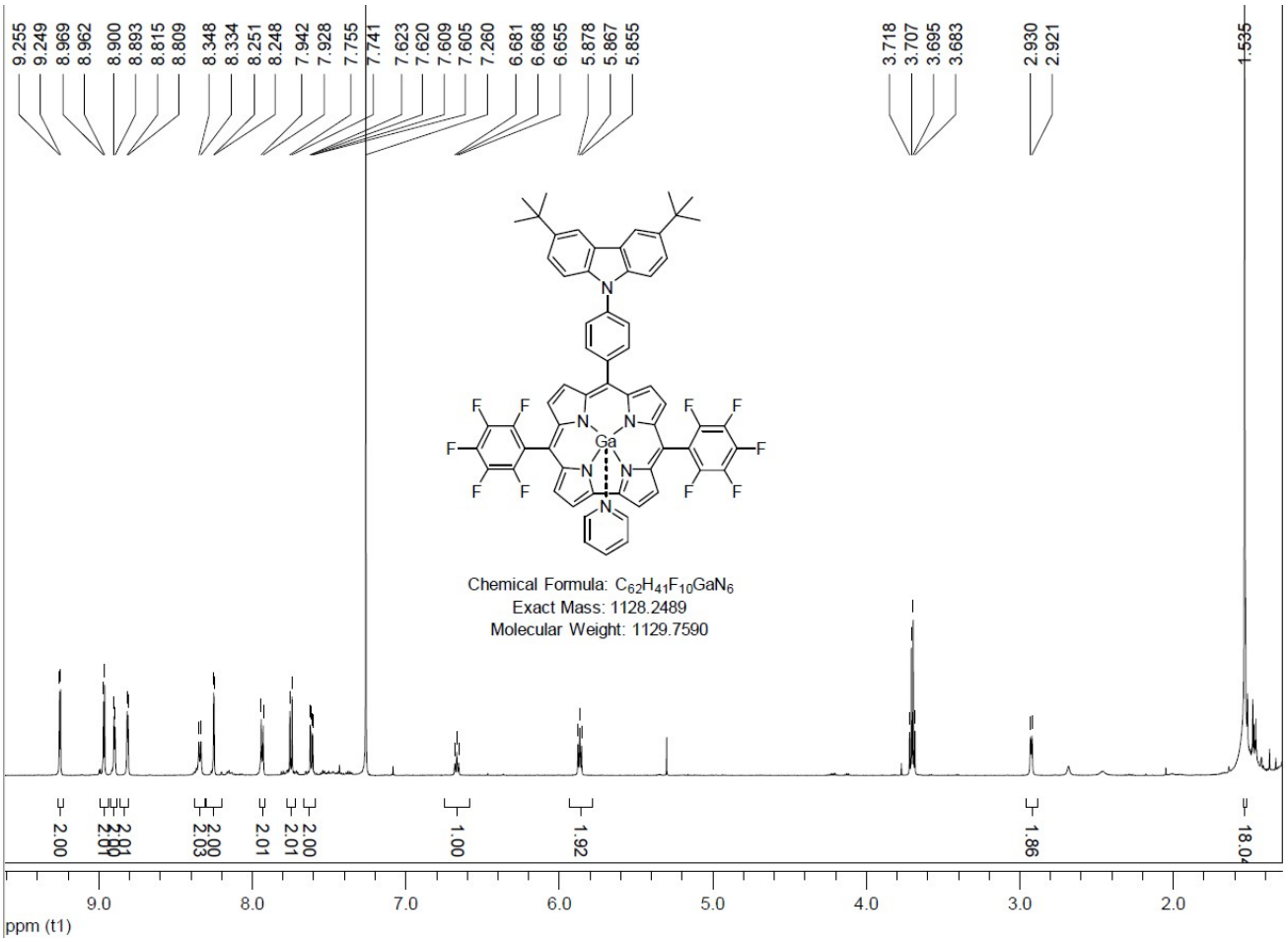

Figure S9. ^{1}H NMR spectrum of **G-1** ($CDCl_3$, 600 M).

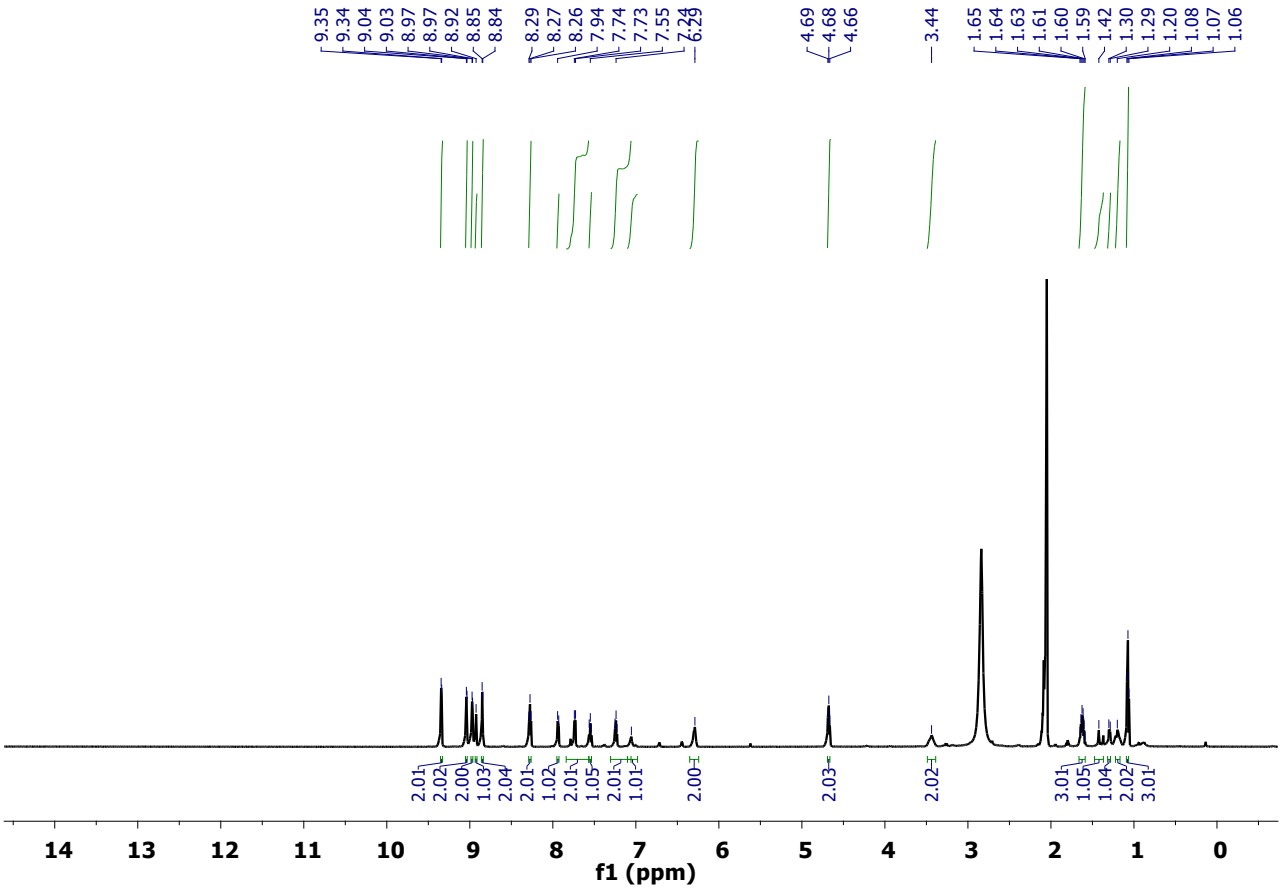

Figure S10. ^{1}H NMR spectrum of **G-2Q** in acetone-d_6.

5. UV-vis absorption spectra in basic media

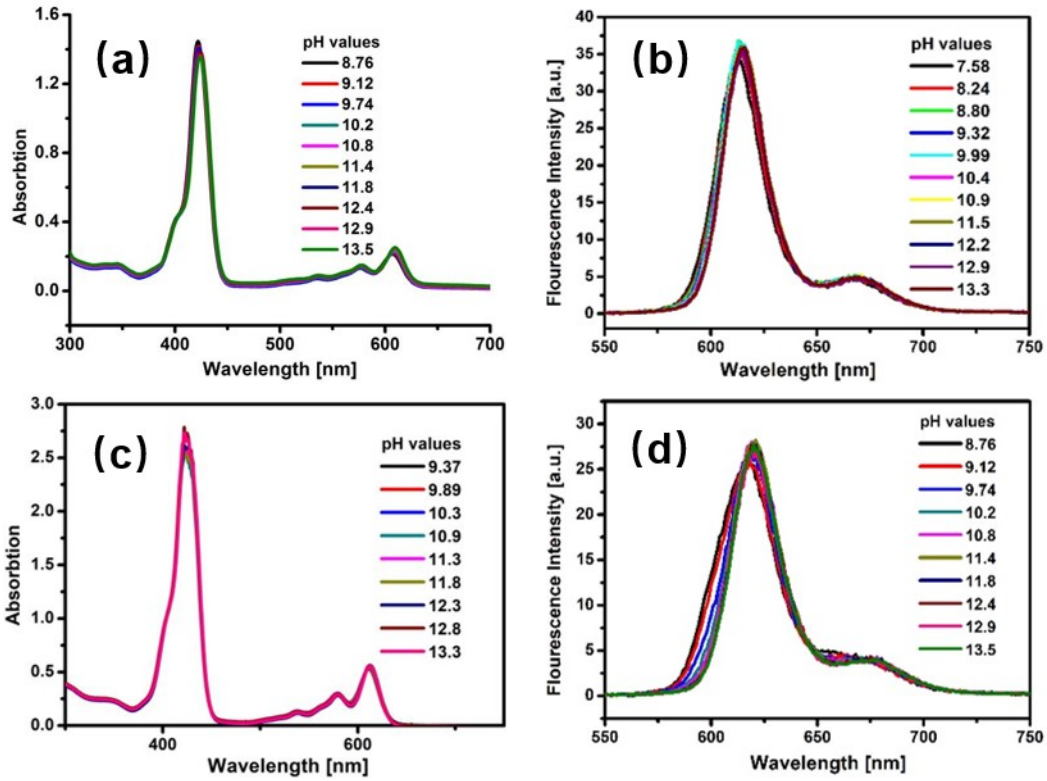

Figure S11. UV-vis absorption (a, c) and fluorescence emission (b, d) spectra of Ga^{III}triarylcorroles **G-1** (a, b) and **G-2** (c, d) under various basic pH conditions.

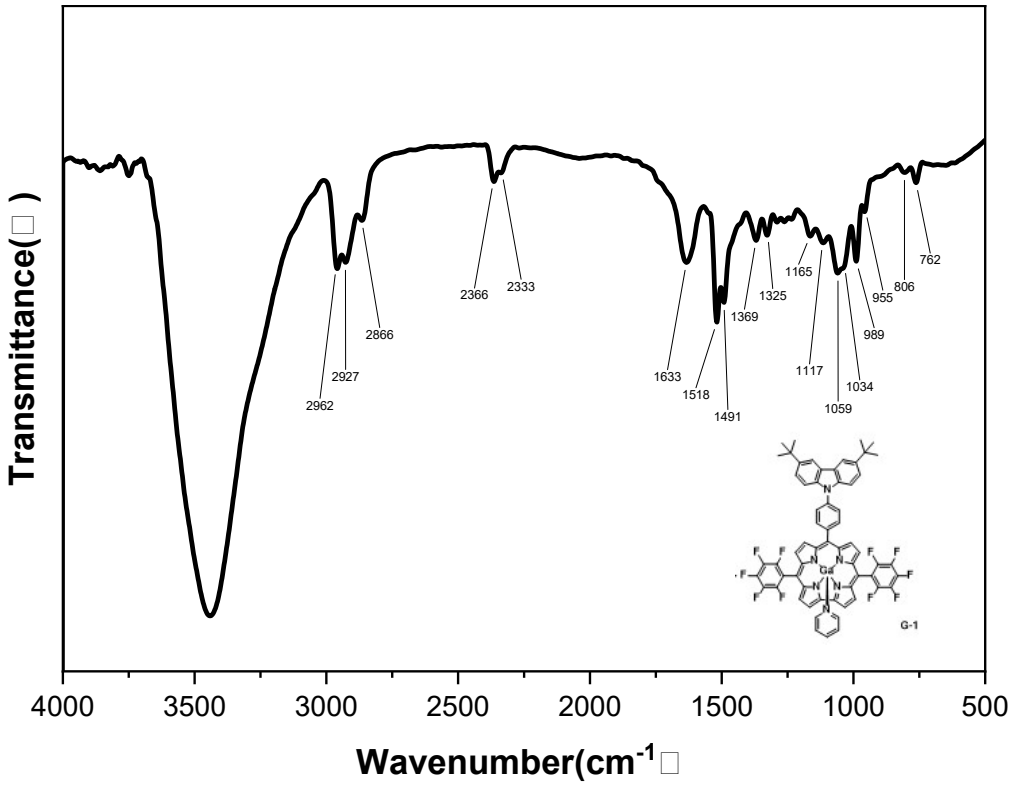

Figure S12. FT-IR spectra of **G-1**

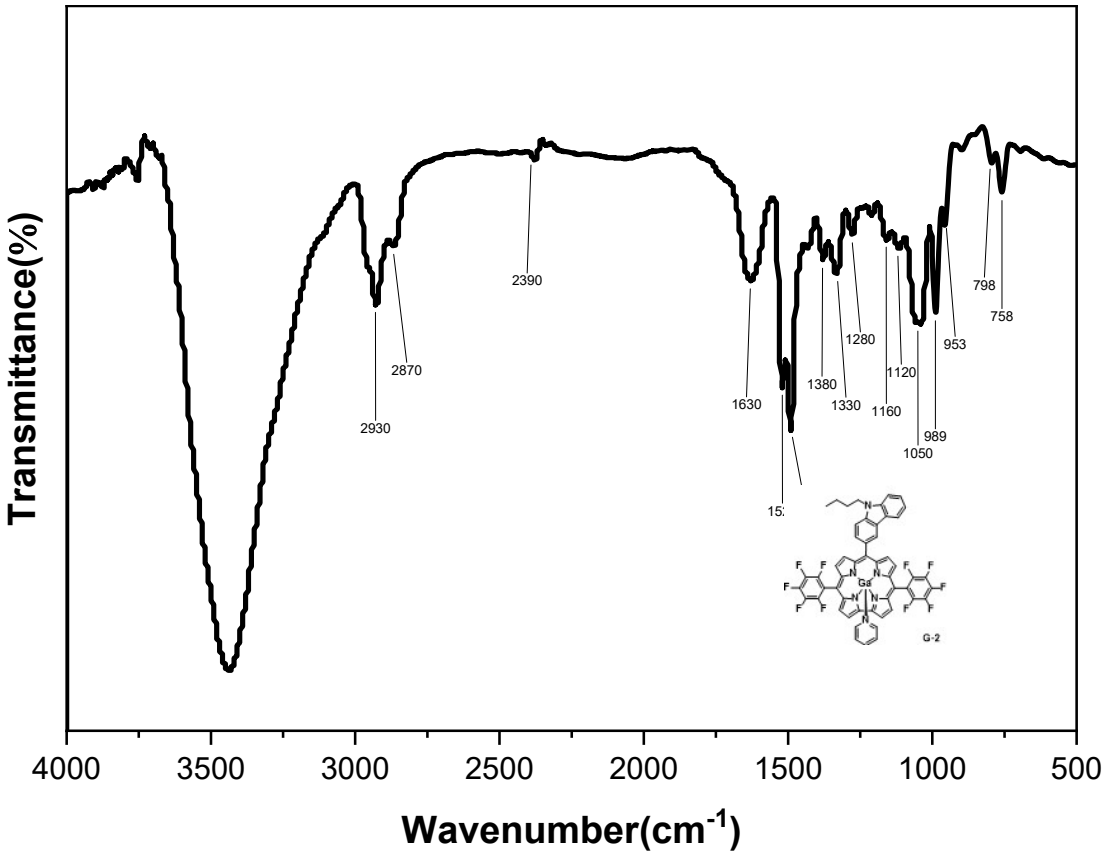

Figure S13. FT-IR spectra of **G-2**

6. **References**

S1. DO Oluwole, E Prinsloo, T Nyokong. Photophysical behavior and photodynamic therapy activity of conjugates of zinc monocarboxyphenoxy phthalocyanine with human serum albumin and chitosan. Spectrochim Acta A 2017;173:292-300. doi: 10.1016/j.saa.2016.09.032

S2. T Mosmann. Rapid colorimetric assay for cellular growth and survival: application to proliferation and cytotoxicity assays. J Immunol Methods 1983;65:55-63. doi: 10.1016/0022-1759(83)90303-4

S3. M Magaraggia, A Visona, A Furlan, A Pagnan, G Miotto, G Tognon, G Jori. Inactivation of vascular smooth muscle cells photosensitized by liposome-delivered Zn (II)–phthalocyanine. J Photochem Photobiol B 2006;82:53-58. doi: 10.1016/j.jphotobiol.2005.08.010

S4. R. C. Soy, B. Babu, J. Mack, T. Nyokong. The photodynamic activities of the gold nanoparticle conjugates of phosphorus(V) and gallium(III) A_3 *meso*-triarylcorroles. Dyes Pigments 2021;194:109631. doi: 10.1016/j.dyepig.2021.109631

S5. JA Arnott, SL Planey. The influence of lipophilicity in drug discovery and design. Expert Opin Drug Discov 2012;7:863-75. doi: 10.1517/17460441.2012.714363

S6. L Kelbauskas, W Dietel. Internalization of Aggregated Photosensitizers by Tumor Cells: Subcellular Time-resolved Fluorescence Spectroscopy on Derivatives of Pyropheophorbide-a Ethers and Chlorin e6 under Femtosecond One-and Two-photon Excitation. Photochem Photobiol 2002;76:686-94. doi: 10.1562/0031-8655(2002)0760686IOAPBT2.0.CO2

S7. C Hansch, PP Maloney, T Fujita, R Muir. Correlation of biological activity of phenoxyacetic acids with Hammett substituent constants and partition coefficients. Nature 1962;194:178-180. doi: 10.1038/194178b0

S8. A. Sindelo, N. Kobayashi, M. Kimura, T. Nyokong. Physicochemical and photodynamic antimicrobial chemotherapy activity of morpholine-substituted phthalocyanines: effect of point of substitution and central metal. J Photochem Photobiol A 2019;374:58-67. doi: 10.1016/j.jphotochem.2019.01.025

S9. B.M. Coffey, G.G., Anderson, 2014. Biofilm formation in the 96-well microtiter plate. In

Pseudomonas methods and protocols. Humana Press, New York, NY, pp. 631-641.

S10. I. Santos, S.R. Gamelas, C. Vieira, M.A. Faustino, J.P. Tomé, A. Almeida, A.T. Gomes, L.M. Lourenço. Pyrazole-pyridinium porphyrins and chlorins as powerful photosensitizers for photoinactivation of planktonic and biofilm forms of E. coli. Dyes Pigments 2021,193:109557. doi: 10.1016/j.dyepig.2021.109557

S11. H. Lade, J.H. Park, S.H. Chung, I.H. Kim, J.M. Kim, H.S. Joo, J.S. Kim. Biofilm formation by Staphylococcus aureus clinical isolates is differentially affected by glucose and sodium chloride supplemented culture media. J. Clinical Med. 2019;8:1853. doi: 10.3390/jcm8111853

S12. Z Zhao, T Nyokong, MD Maree. Synthesis and photochemical characterization of a zinc phthalocyanine–zinc porphyrin heterotrimer and heterononamer. Dalton Trans 2005;23:3732-7. doi: 10.1039/B508478D

S13. N Gandra, AT Frank, O Le Gendre, N Sawwan, D Aebisher, JF Liebman, KN Houk, A Greer, R Gao. Possible singlet oxygen generation from the photolysis of indigo dyes in methanol, DMSO, water, and ionic liquid, 1-butyl-3-methylimidazolium tetrafluoroborate. Tetrahedron 2006;62:10771-6. doi: 10.1016/j.tet.2006.08.095

S14. MJ Frisch, GW Trucks, HB Schlegel, GE Scuseria, MA Robb, JR Cheeseman, G Scalmani, V Barone, B Mennucci, GA Petersson, H Nakatsuji, M Caricato, X Li, HP Hratchian, AF Izmaylov, J Bloino, G Zheng, JL Sonnenberg, M Hada, M Ehara, K Toyota, R Fukuda, J Hasegawa, M Ishida, T Nakajima, Y Honda, O Kitao, H Nakai, T Vreven, JA Montgomery, Jr, JE Peralta, F Ogliaro, M Bearpark, JJ Heyd, E Brothers, KN Kudin, VN Staroverov, R Kobayashi, J Normand, K Raghavachari, A Rendell, JC Burant, SS Iyengar, J Tomasi, M Cossi, N Rega, JM Millam, M Klene, JE Knox, JB Cross, V Bakken, C Adamo, J Jaramillo, R Gomperts, RE Stratmann, O Yazyev, AJ Austin, R Cammi, C Pomelli, JW Ochterski, RL Martin, K Morokuma, VG Zakrzewski, GA Voth, P Salvador, JJ Dannenberg, S Dapprich, AD Daniels, Ö Farkas, JB Foresman, JV Ortiz, J Cioslowski, DJ Fox, Gaussian, Inc., Wallingford CT, 2009.